

Spin exchange interaction with tunable range between graphene quantum dotsMatthias Braun,^{*} P. R. Struck, and Guido Burkard[†]*Institute of Theoretical Physics C, RWTH Aachen University, D-52056 Aachen, Germany and**Department of Physics, University of Konstanz, D-78457 Konstanz, Germany*

(Received 12 November 2010; revised manuscript received 4 July 2011; published 23 September 2011)

We study the spin exchange between two electrons localized in separate quantum dots in graphene. The electronic states in the conduction band are coupled indirectly by tunneling to a common continuum of delocalized states in the valence band. As a model, we use a two-impurity Anderson Hamiltonian which we subsequently transform into an effective spin Hamiltonian by way of a two-stage Schrieffer-Wolff transformation. We then compare our result to that from a Coqblin-Schrieffer approach as well as to fourth-order perturbation theory.

DOI: [10.1103/PhysRevB.84.115445](https://doi.org/10.1103/PhysRevB.84.115445)

PACS number(s): 73.22.Pr, 75.30.Et, 03.67.Lx, 75.70.-i

I. INTRODUCTION

Spins in quantum dots (QDs) are under intense investigation as a possible realization of qubits.¹ Among the currently most advanced solid-state structures are top-gate-patterned two-dimensional electron gases in GaAs heterostructures.² However, in this host material hyperfine interaction between the spin of the electron and that of the atomic nuclei of the host material leads to relatively short coherence times. A promising way to circumvent this problem is the use of carbon as a host material for spin qubits. Natural carbon comprises 99% of the carbon isotope ¹²C, which has no nuclear spin. This gives carbon-based devices the advantage that decoherence due to hyperfine interaction is suppressed by the small abundance of nuclear spins. Carbon is also a relatively light element, therefore spin-orbit coupling is expected to be weaker than in GaAs. One can expect a significant improvement of spin coherence times in carbon-based structures. Graphene³ is a promising host material for spin qubits.^{4,5} It naturally creates a perfect confinement of electrons in one dimension. Moreover, in contrast to carbon nanotubes,^{6,7} the ability to lithographically pattern graphene allows for a deterministic device preparation, which is necessary for scalability.¹ Graphene has a very interesting electronic structure, with a gapless and linear dispersion around the Fermi energy. Furthermore, the electronic eigenstates carry an additional internal degree of freedom, dubbed pseudospin, which is always aligned with the direction of the momentum. These properties imitate the behavior of relativistic chiral massless Dirac particles.⁸ These relativistic-like properties lead to the phenomenon of Klein tunneling,⁹ which actually prohibits any electrostatic confinement of electrons, i.e., the formation of QDs.

Among the most promising ideas for overcoming Klein tunneling is to use graphene nanoribbons or constrictions instead of extended graphene as host material^{4,10–12} (see Fig. 1). In clean graphene nanoribbons with armchair boundaries, the additional confinement can lead to the opening of a small energy gap at the Fermi energy.¹³ The size of the gap is inversely proportional to the width of the ribbon. In the presence of such a gap, the pseudorelativistic behavior of the charge carriers is lost, and the material resembles a regular gaped semiconductor, enabling electrostatic confinement.⁴ However, it has been shown both experimentally and theoretically that

rough edges are sufficient to open up a gap. As a side effect, the sharp edges also lift the valley degeneracy in bulk graphene, which could suppress the Heisenberg spin interaction between the QDs.⁴

The exchange interaction has been identified as an underlying mechanism to mediate the necessary interactions for two-qubit gates among spin qubits.^{1,14} The Heisenberg exchange coupling between spins \mathbf{S}_i is described by the Hamiltonian $H = \sum_{\langle ij \rangle} J_{ij} \mathbf{S}_i \cdot \mathbf{S}_j$ and provides a pairwise coupling between adjacent spin qubits i and j . In the context of quantum-computational applications it is also necessary to couple qubits which are not nearest neighbors. Long-range spin-spin interactions can, e.g., be mediated by cavity photons.¹⁵ Here, we investigate the coupling between two spin qubits in a graphene nanoribbon via the valence band. We find that this coupling has a tunable range and can be used to couple distant QD spins.

Following Ref. 4, we consider a system as shown in the upper part of Fig. 1, where several electric gates are placed on top of an armchair nanoribbon. By applying a gate voltage, the dispersion relation of the material below the gates can be shifted in energy (see the lower part of Fig. 1). If, at a certain energy, extended states can exist in one section, but not in the neighboring ribbon sections, additional size quantization along the ribbon leads to single localized states. In the energy interval above and below the gap, the states are extended and form a continuum. With a suitable adjustment of the chemical potential, the localized states can be filled with one electron each, forming a one-dimensional array of qubits. In the following, we calculate the Heisenberg spin interaction between two such spin qubits.

The RKKY interaction¹⁶ between localized magnetic moments is well discussed for extended graphene (see Refs. 17 and 18) and, after the experimental discovery of graphene, revisited in Refs. 19–23. Here, we study a graphene nanoribbon where a gap opens at the Fermi energy. Due to this gap, the spin exchange problem we are interested in resembles less the one in extended graphene and more the case in ordinary semiconductors in reduced dimensions,^{24–26} like quantum wells²⁷ or quantum wires.²⁸ However, compared to conventional semiconductors, the band gap can be unusually small, of the order of 1–100 meV. Therefore, by applying

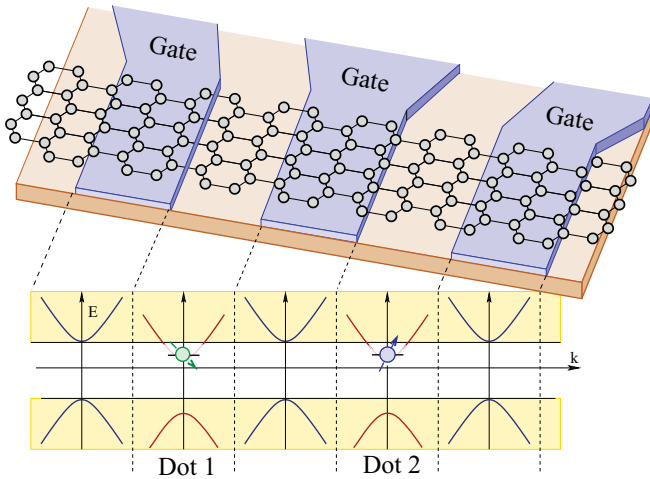


FIG. 1. (Color online) One-dimensional quantum dot array on an armchair graphene nanoribbon (drawing not to scale). Due to the ribbon structure, the dispersion relation of graphene can exhibit a gap, which scales inversely with the ribbon width. This gap allows for electrostatic confinement of electrons in quantum dots. As the band gap is small compared to regular semiconductors, the spin exchange mechanism between the quantum dots is not dominated by RKKY-type processes alone, and superexchange processes contribute significantly.

gate voltages, one can realize an arbitrary alignment of the QD energy level relative to the valence and conduction band. Due to the proximity of the band edges of the valence and/or conduction band, the band edges must be taken into account.²⁹

II. TRANSFORMATION OF THE HAMILTONIAN

A. Model

We model the system as two Anderson impurities, which are both in contact with a common energy band. The Hamiltonian for our model is

$$H = H_0 + H_T, \quad (1)$$

$$H_0 = \sum_{i=1,2} \left(\sum_{\sigma=\uparrow,\downarrow} \varepsilon_i a_{i\sigma}^\dagger a_{i\sigma} + U_i a_{i\uparrow}^\dagger a_{i\uparrow} a_{i\downarrow}^\dagger a_{i\downarrow} \right) + \sum_{k\sigma} \varepsilon_k c_{k\sigma}^\dagger c_{k\sigma}, \quad (2)$$

$$H_T = \sum_{ik\sigma} (t_{ik}(\mathbf{r}_i) c_{k\sigma}^\dagger a_{i\sigma} + t_{ik}^*(\mathbf{r}_i) a_{i\sigma}^\dagger c_{k\sigma}). \quad (3)$$

The first part of H_0 describes the two independent QDs, $i = 1, 2$, containing one electronic level each. The fermionic operators $a_{i\sigma}$ and $a_{i\sigma}^\dagger$ create and annihilate electrons on dot i with spin σ . Due to the low electrostatic capacity of a QD, double occupation of one individual dot is associated with a substantial charging energy U_i . For quantum computation applications one is interested in a parameter regime where the QDs are occupied with one electron each to form a spin-1/2 qubit.

The second part of H_0 models the contacting continuum of states as a large reservoir of noninteracting electrons. Here $c_{k\sigma}, c_{k\sigma}^\dagger$ denote the annihilation and creation operators for electrons in the continuum with (orbital) quantum numbers k and spin σ . The continuum is assumed to be unpolarized and at zero temperature (filled valence band). The tunneling Hamiltonian H_T describes spin-conserving tunneling between the two dots and the continuum. The tunnel amplitudes $t_{ik}(\mathbf{r}_i)$ depend on the dot and the continuum quantum numbers i and k , as well as on the position \mathbf{r}_i of the QDs. However, the exact form of $t_{ik}(\mathbf{r}_i)$ depends on the system under consideration.

The two-impurity Anderson model and the strongly related Anderson lattice model is extensively discussed in the literature.^{30–43} The ansatz we use was originally proposed by Coqblin and Schrieffer in Ref. 44.

B. Schrieffer-Wolff transformation

Following Refs. 39, 40, and 45, we use a two-stage or nested Schrieffer-Wolff transformation to derive an effective spin Hamiltonian. In contrast to previous works, we do not assume equal energy levels in the two Anderson impurities, as the confinement of the QDs can be modified individually. By keeping track of the dot indices it is also possible to identify different physical processes in the final result, and enables us to compare our result to higher-order perturbation theory.

The Schrieffer-Wolff transformation^{42,46–48} is based on a canonical transformation of the Hamiltonian, $H^{(1)} = e^{iS} H e^{-iS} = H + [iS, H] + \frac{1}{2}[iS, [iS, H]] + \dots$. The division of the Hamiltonian H into a free Hamiltonian H_0 and a small perturbation H_T allows us to choose a transformation S_1 , fulfilling the relation $[iS_1, H_0] = -H_T$ and leading us to the effective Hamiltonian $H^{(1)} = H_0 + \frac{1}{2}[iS_1, H_T] + \frac{1}{3}[iS_1, [iS_1, H_T]] + \frac{1}{6}[iS_1, [iS_1, [iS_1, H_T]]] + \dots$, where the lowest-order tunneling term is canceled. Since S also has to be of first order in the tunneling amplitudes, $S_1 \propto H_T$, the interaction now appears (at least) in second order. Please see Appendix A for details on the first Schrieffer-Wolff transform.

By a subsequent Schrieffer-Wolff transformation with the generator S_2 fulfilling $[iS_2, H_0] = -\frac{1}{2}[iS_1, H_T]$, the second-order interaction term can also be removed. Note that now $S_2 \propto H_T^2$. At the end we project the resulting Hamiltonian on the subspace where both QDs are occupied by one electron. As all odd-order interactions do not conserve the occupation numbers of the QD, they can be neglected, as they will be projected out at the end of the calculation. Combining both steps, we arrive at the effective Hamiltonian

$$H^{(2)} = H_0 + \frac{1}{4}[iS_2, [iS_1, H_T]] + \frac{1}{8}[iS_1, [iS_1, [iS_1, H_T]]], \quad (4)$$

where corrections in sixth and higher orders in the tunneling amplitudes have been neglected. After projecting out the continuum degrees of freedom, and in addition to unimportant level renormalizations, which we do not discuss, we find a Heisenberg-like interaction, $J \mathbf{S}_1 \cdot \mathbf{S}_2$, which couples the two QD spins $\mathbf{S}_i = \sum_{\alpha\beta} a_{i\alpha}^\dagger \boldsymbol{\sigma}_{\alpha\beta} a_{i\beta}$, consistent with Refs. 39 and 50. A detailed calculation is presented in Appendix B. After nontrivial regrouping of terms,⁵¹ one can separate the spin interaction into parts originating from different virtual tunneling processes defined by their intermediate virtual

quantum state with the explicit shape

$$J = 2 \sum_{k,q} t_{1,k}^* t_{2,k} t_{1,q} t_{2,q}^* e^{i(k-q) \cdot (R_1 - R_2)} (J_1 + J_2 + J_3 + J_4), \quad (5)$$

$$J_1 = \left(\frac{1}{\varepsilon_k - \varepsilon_1} - \frac{1}{\varepsilon_q - \varepsilon_1 - U_1} \right) \frac{n_k - n_q}{\varepsilon_k - \varepsilon_q} \left(\frac{1}{\varepsilon_q - \varepsilon_2} - \frac{1}{\varepsilon_k - \varepsilon_2 - U_2} \right), \quad (6)$$

$$J_2 = \left(\frac{1}{\varepsilon_k - \varepsilon_1} + \frac{1}{\varepsilon_q - \varepsilon_2} \right) \frac{1 - n_q}{\varepsilon_k + \varepsilon_q - \varepsilon_1 - \varepsilon_2} \left(\frac{1}{\varepsilon_q - \varepsilon_1} + \frac{1}{\varepsilon_k - \varepsilon_2} \right), \quad (7)$$

$$J_3 = \left(\frac{1}{\varepsilon_1 + U_1 - \varepsilon_k} + \frac{1}{\varepsilon_2 + U_2 - \varepsilon_q} \right) \frac{+n_q}{\varepsilon_1 + U_1 + \varepsilon_2 + U_2 - \varepsilon_k - \varepsilon_q} \left(\frac{1}{\varepsilon_1 + U_1 - \varepsilon_q} + \frac{1}{\varepsilon_2 + U_2 - \varepsilon_k} \right), \quad (8)$$

$$J_4 = \left(\frac{1}{\varepsilon_k - \varepsilon_1} + \frac{1}{\varepsilon_k - \varepsilon_2 - U_2} \right) \frac{-n_q}{\varepsilon_2 + U_2 - \varepsilon_1} \left(\frac{1}{\varepsilon_q - \varepsilon_1} - \frac{1}{\varepsilon_q - \varepsilon_2 - U_2} \right) + \frac{1}{\varepsilon_k - \varepsilon_1} \frac{+1}{\varepsilon_2 + U_2 - \varepsilon_1} \frac{1}{\varepsilon_q - \varepsilon_1} + (1 \leftrightarrow 2). \quad (9)$$

The first term J_1 resembles an RKKY interaction.¹⁶ The interaction is mediated by a virtual particle-hole excitation in the electron gas [see Fig. 2(a)]. Therefore the energy of the intermediate excitation is given by $\varepsilon_q - \varepsilon_k$. The second and third contributions to the spin-spin interaction originate from virtual two-particle(hole) excitations in the continuum Fermi sea [see Figs. 2(b) and 2(c)]. Two electrons tunnel coherently from or to the QDs. Thus, as intermediate virtual states, the two QDs are both doubly occupied (empty). Afterward, the electrons tunnel crosswise back, interchanging the spins of the QDs. This process leads to the interactions J_2 and J_3 .

Finally, the last contribution J_4 is caused by the possibility of direct tunneling of one dot electron to the other dot. The virtual intermediate state is therefore one double-occupied dot and one empty dot. The tunneling can happen through filled as well as empty states in the electron gas [see Fig. 2(d)].

C. Relation to Coqblin-Schrieffer model

In Ref. 44 Coqblin and Schrieffer present their widely used approach^{31,52} to the two-impurity Anderson model. They perform a single Schrieffer-Wolff transformation and project the resulting Hamiltonian of the single-occupied impurities. With this, they transform the two individual Anderson models into two individual s - d models or Kondo impurities. The spin of one QD S_i is coupled to the bath electron spins by

$$H_{\text{Kondo}} = \sum_{kq,\sigma\sigma'} J_{kq}^i S_i \cdot c_{k\sigma}^\dagger \sigma_{\sigma\sigma'} c_{q\sigma'}, \quad (10)$$

see Appendix A for details. By treating that Hamiltonian in second-order perturbation theory, they compute a RKKY-like spin-spin interaction¹⁶ of the form

$$\sum_{kq} J_{kq}^1 J_{kq}^2 \frac{n_k - n_q}{\varepsilon_k - \varepsilon_q} S_1 \cdot S_2. \quad (11)$$

Even though Eq. (11) captures the basic features of Eq. (6), it is an expansion inconsistent in the order of the tunnel amplitudes. First, the initial Schrieffer-Wolff transformation generates not only terms of second order, but also the term $[iS_1, [iS_1, [iS_1, H_T]]]$, which contributes in fourth order⁴¹ [see

Eq. (4)]. Actually contributions from this higher order term cancel several parts in Eq. (11), leading to Eq. (6). By truncating the transformation at second order, these contributions to the spin interaction are lost.

Second, the initial Schrieffer-Wolff transformation generates not only the Kondo-Hamiltonian, but also terms in second order of the form $a_1^\dagger a_2$, which describe direct tunneling between the two QDs.⁴⁹ In a subsequent second-order perturbation theory, these terms also lead to an interdot spin interaction. In Ref. 44 these interactions are neglected due to the premature projection of the result of the Schrieffer-Wolff transformation on the single occupied dot subspace.

Interestingly, in the limit of energy levels far away from the Fermi energy, i.e., when one assumes that the spin coupling J_{kq}^i approaches a constant, the Coqblin-Schrieffer approach generates the correct result. However, nowadays the Anderson model is extensively used to describe QDs.²⁸ In contrast to rare earth compounds or true atomic systems, the typical energy scale of the QD level spectrum is several orders of magnitude smaller. Therefore in these artificial systems the application of the Coqblin-Schrieffer model needs to be handled with care.

D. Relation to fourth-order perturbation theory

Starting from the two-impurity Anderson model, one can also derive a fourth-order dot spin-spin interaction by perturbation theory,^{32,34,38,53} with or without diagrammatical help. The perturbation approach nearly reproduces our results Eqs. (6)–(9) with one exception: the structure of the Fermi functions. Via perturbation theory, one would expect, for example, that the two-lead-particle excitation [see Fig. 2(c)] only happens if the two electron gas states k and q are empty; therefore the spin coupling J_2 should be proportional to $(1 - n_k)(1 - n_q)$. In contrast, the contribution from a Schrieffer-Wolff transformation is proportional to $(1 - n_q)$ and independent of n_k . By counting the operator commutators, one can directly determine that the spin-spin coupling derived by a two-stage Schrieffer-Wolff transformation cannot generate terms that contain four lead operators, which would be necessary for a product term like $n_k n_q$. The reason for this discrepancy between fourth order perturbation theory

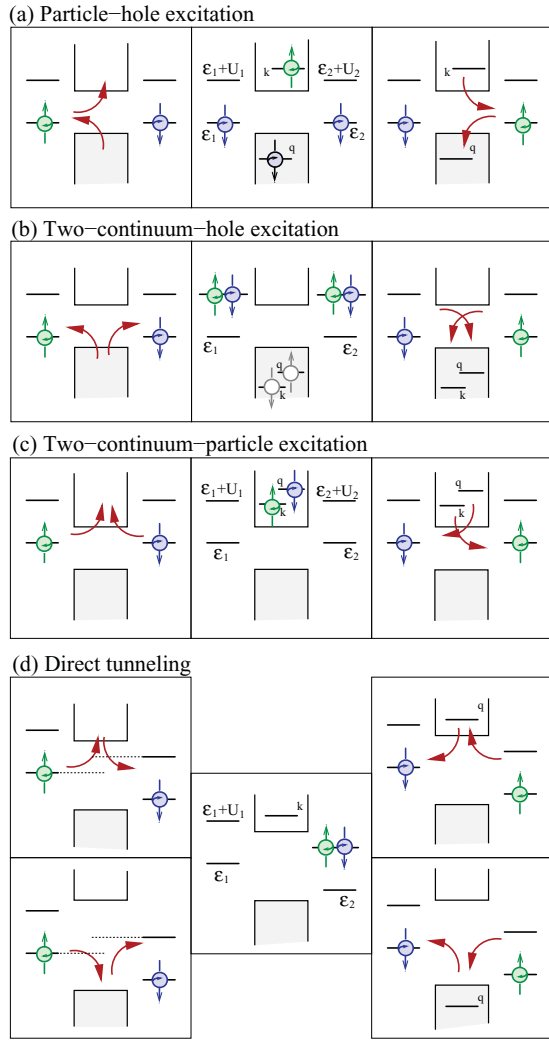


FIG. 2. (Color online) Several virtual tunnel processes contribute to the spin-spin interaction between the dots. These processes can be classified by the intermediate state of the system. While particle-hole excitation (a) leads to an RKKY-like interaction, processes (b–d) are usually summarized as superexchange.

and Schrieffer-Wolff transformation lies in the procedure of integrating out the lead degrees of freedom, i.e., by the replacement of the thermal average of lead operators $\langle c_k^\dagger c_k \rangle_{\text{th}}$ by the Fermi function n_k . In the case of the perturbation theory, the operators c_k^\dagger, c_k refer to the bare unperturbed electronic states of the lead, i.e., one assumes that the lead is actually not perturbed by tunneling. After the Schrieffer-Wolff transformation, the lead operators refer to new lead states, which are hybridized with the localized dot states. By performing the thermal average, one therefore assumes that these new hybridized lead states are in thermal equilibrium, not the bare lead states. Therefore, it is not surprising that the results of a Schrieffer-Wolff transformation and perturbation theory differ. However, it is surprising that one can express the result of the Schrieffer-Wolff transformation in the same functional form one would expect from perturbation theory, except for the Fermi functions. Only due to this structure of terms one actually can, in

the spirit of Feynman diagrams, assign virtual processes as shown in Fig. 2. For this reason, the grouping of terms in Eqs. (6)–(9) is physically plausible but, to some extent, arbitrary.

III. APPLICATION TO GRAPHENE NANORIBBON QUANTUM DOTS

Up to now, the computed result in Eqs. (6)–(9) is general for the spin coupling of two qubits by a common continuum of states labeled by the indices k and q . In the following, we specify this continuum to the electronic structure of a graphene nanoribbon aligned along the y direction.

A. Band structure

Bulk graphene has two independent Fermi points at the momenta \mathbf{K} and \mathbf{K}' in reciprocal space, generating the valley degeneracy. Due to the armchair boundary conditions of the ribbon, the propagating wave states with momentum $\mathbf{K} + \mathbf{k}$ and $\mathbf{K}' + \mathbf{k}$ are coupled.^{13,54} The confinement in the x direction leads to a further quantization of the transverse wave vector $k_x \equiv k_n = (n \pm 1/3)\pi/W$, with W denoting the ribbon's width and $n \in \mathbb{N}$. Therefore the continuum states can be characterized by the sub-band index n and the momentum component $k_y \equiv k$ along the ribbon. Close to the Fermi energy, the dispersion relations becomes

$$\varepsilon_{k,n} = \hbar v_F \sqrt{k^2 + k_n^2}, \quad (12)$$

with the Fermi velocity v_F of graphene. This dispersion resembles the dispersion of a massive relativistic particle.

The transverse confinement determines the energy gap $2\varepsilon_g = 2\hbar v_F k_0$, which scales inversely with the ribbon width.⁵⁵ Due to this gap, electrons can be confined by electrostatic gates, in analogy to conventional semiconductors.⁴ We assume the applied electric potential to be independent of the x coordinate (see Fig. 1), therefore the band index n is conserved. Therefore we only need to consider the continuum sub-band with the same band index as the bound state(s). Even if this symmetry is broken, the generalization to multi-sub-bands is straightforward.⁷ As a further simplification, we assume that by applying electrostatic gates, the dispersion relation of the extended states is still described by Eq. (12).

B. Tunnel amplitudes

The spin exchange is proportional to the product of the four tunnel amplitudes $t_{1,k}^*(\mathbf{r}_1)t_{2,k}(\mathbf{r}_2)t_{1,q}(\mathbf{r}_1)t_{2,q}^*(\mathbf{r}_2)$. In analogy to most cases studied in the literature, we assume that the amplitude of the overlap of the bound states and the extended states does not explicitly depend on the momentum k of the extended states. This assumption is valid if the wave function of the bound state is localized on a length scale smaller than the wavelength of the extended state. However, in QDs in semiconductors in general, and in particular in the vicinity of a band edge, this assumption may not be valid. As k -independent tunnel amplitudes lead to a shorter spin exchange range, the spin exchange range derived in the following can be seen only as a lower bound. Although the magnitude of the tunnel amplitude does not depend on k within this approximation,

the fact that the two QDs are separated in space gives rise to a relative phase. While in ordinary isotropic metals this phase is simply given by $e^{ik \cdot r_i}$, in graphene the valley degeneracy has to be taken into account. In nanoribbons, the energy eigenstates are phase-locked superpositions of the states of both valleys. Therefore, the overlap of the wave functions^{4,54} leads to a tunnel amplitude of the form

$$t_{1,k}(\mathbf{r}_1) = t_1 e^{-ik \cdot \mathbf{r}_1} \frac{e^{-i\mathbf{K} \cdot \mathbf{r}_1} + e^{-i\mathbf{K}' \cdot \mathbf{r}_1}}{\sqrt{2}}. \quad (13)$$

The spin coupling therefore will always contain a contribution which oscillates on inter-atomic distances and one contribution which varies on the length scale of the envelope wave function. As the QDs under consideration are not spatially defined with lattice site precision, we expect that the oscillating contribution to the spin exchange will average out.

C. Spin-exchange range

Which of the virtual tunnel processes (see Fig. 2) dominates the spin exchange between two QDs depends on the alignment of the dot energy levels, band gap, and edges. Roughly speaking, the virtual process requiring the lowest excitation energy will dominate. As we assume the graphene nanoribbon to be nearly undoped, the Fermi energy of the system lies within the band gap. Therefore the valence band is entirely filled, and the conduction band is empty. The RKKY-like exchange interaction via a particle-hole excitation in the continuum will be suppressed by the band gap $2\varepsilon_g$, and superexchange processes will dominate. In order to maximize the nonlocal exchange between remote spins, we focus on the scenario shown in Fig. 3, where the QD level lies close to the valence band, and the charging energy is smaller than the band gap.

In this level alignment, direct tunneling processes via the valence band dominate the spin exchange. The resulting

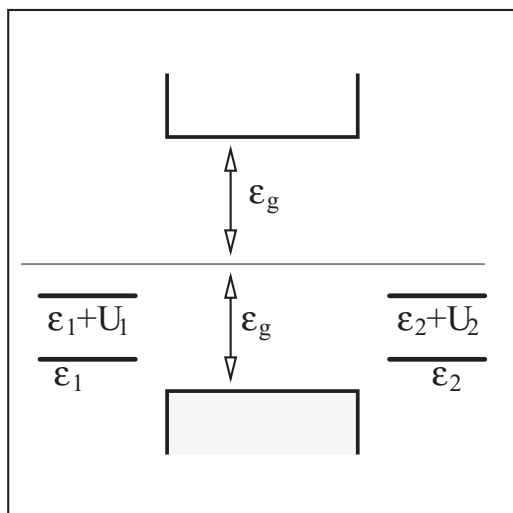


FIG. 3. If the quantum dot level lies close to the valence band, and the charging energy is lower than the band gap, direct tunneling processes will dominate the spin exchange between the quantum dots.

integrals can be computed by Cauchy's integral formula. The exchange due to direct tunneling turns out to be

$$J = -\frac{|t_1|^2 |t_2|^2}{4\Delta E^2} \frac{1}{\varepsilon_2 + U_2 - \varepsilon_1} \frac{(\varepsilon_2 + U_2)^2}{\varepsilon_g^2 - (\varepsilon_2 - U_2)^2} \times e^{-2\sqrt{\frac{\varepsilon_g^2 - (\varepsilon_2 + U_2)^2}{\hbar v_F}} \Delta r} + (1 \leftrightarrow 2), \quad (14)$$

with the QD distance $\Delta r = |\mathbf{r}_1 - \mathbf{r}_2|$. The energy $\Delta E = \hbar v_F/L$ is the energy splitting of the continuum states, with L being the length of the ribbon. As the tunnel amplitudes t_i decrease with the real-space particle density of the band states with $1/\sqrt{L}$, the strength of the spin exchange is independent of the overall length of the ribbon.

The strength of the spin coupling driven by direct tunneling diverges within fourth order, if the single-occupied state of one dot becomes resonant with the double-occupied state of the other dot. The range $\lambda = \hbar v_F/2\sqrt{\varepsilon_g^2 - (\varepsilon_2 + U_2)^2}$ of the coupling Eq. (14) on the other side is controlled by the energy separation between the double-occupied state of the one dot and the valence band edge at energy $-\varepsilon_g$. If one assumes that the single-occupied states of the two dots are close to the band edge ($\varepsilon_g \approx \varepsilon_i$), the exchange range scales as $\hbar v_F/\sqrt{8\varepsilon_g U_i}$. For a graphene nanoribbon with a width of 50 nm and a QD with a charging energy of 4 meV,¹¹ this length is of order 50 nm, i.e., comparable to the QD length.

If one assumes that, in analogy to a capacitor, the charging energy of a QD scales inversely with its area,¹¹ then the range of the spin exchange interaction scales linearly with the width of the nanoribbon.

D. Further considerations

The lower bound for the spin exchange range between QDs in a graphene nanoribbon is given by the ribbon width. For this result we considered only virtual tunnel processes via free continuum states. In addition, also direct tunneling between the QD states can occur. If the QD level approaches the band gap, the bound electron leaks further and further into the barrier due to the weakening of the confinement. Therefore it can happen that two neighboring QD wave functions can acquire a nonvanishing overlap, and direct tunneling becomes possible. Direct tunneling is accompanied also by a spin-exchange interaction.⁴

Furthermore, we have assumed so far that the graphene nanoribbon is infinitely long. This assumption is hidden in the approach to treat the continuum states with momentum k independent of the state $-k$. However, if a finite ribbon length leads to a defined phase relation of the forward and backward propagating states, then one part of the tunnel amplitude will become entirely independent of the momentum k and, therefore, on the distance Δr .⁴ (cf. also the discussion in Sec. III B.) In this case, the range λ of the spin exchange is not determined by the dephasing of the exchange contributions of different states within the Fermi sea, but only by the phase coherence length of the extended states.

IV. CONCLUSIONS

In this paper, we have discussed the spin exchange between localized states which are only indirectly coupled via a continuum of states. Using a two-stage Schrieffer-Wolff transformation, we transformed a two-impurity Anderson model into an effective spin Hamiltonian. Based on our result, we discussed the validity of the Coqblin-Schrieffer approach to this problem. Furthermore, by reordering the terms, we were able to directly compare the Schrieffer-Wolff result to perturbation theory and observe distinct differences that originate from different assumptions on the continuum of states.

As an application of the formalism developed here, we discussed the spin exchange interaction between electrostatically confined QDs in a graphene nanoribbon, as shown in Eq. (14). As a lower bound, we derive a range of this spin exchange of the order of the nanoribbon width. However, the dot energies can be adjusted in such a way as to extend the exchange coupling to longer distances.

ACKNOWLEDGEMENT

We acknowledge funding from the DFG within FOR 912 and within SFB 767.

APPENDIX A: FIRST SCHRIEFFER-WOLFF TRANSFORMATION

The generator of the first Schrieffer-Wolff transformation must fulfill the relation $[iS_1, H_0] = -H_T$. As the part of the Hamiltonian H_0 only contains number operators, i.e., is quadratic or quartic in the fermion operators, one can deduce that iS must have the same structure as the tunnel Hamiltonian H_T , up to a prefactor containing either constants or number operators. With such an ansatz, the generator of the first Schrieffer-Wolff transformation is found to be

$$\begin{aligned} iS_1 &= \sum_{i,k,\sigma} \frac{t_{i,k}}{\varepsilon_k - \varepsilon_i - U_i n_{i\bar{\sigma}}} c_{k\sigma}^\dagger a_{i\sigma} - \frac{t_{i,k}^*}{\varepsilon_k - \varepsilon_i - U_i n_{i\bar{\sigma}}} a_{i\sigma}^\dagger c_{k\sigma} \\ &= \sum_{i,k,\sigma} t_{i,k} \left[\frac{1 - n_{i\bar{\sigma}}}{\varepsilon_k - \varepsilon_i} + \frac{n_{i\bar{\sigma}}}{\varepsilon_k - \varepsilon_i - U_i n_{i\bar{\sigma}}} \right] c_{k\sigma}^\dagger a_{i\sigma} - \text{h.c.} \end{aligned} \quad (\text{A1})$$

This transformation removes the interaction term of first order in the tunneling amplitude and, instead, generates higher

order interactions starting at the second order of t . The new interaction Hamiltonian $H_T^{(1)} = \frac{1}{2}[iS_1, H_T] + O(t^3)$ becomes

$$\begin{aligned} H_T^{(1)} &= \sum_{i,k,q,\sigma} J_{kq}^i \mathbf{S}_i \cdot \mathbf{s}_{kq} + \frac{-1}{2} \sum_{ij,k,\sigma} A_{ij}^k a_{i\sigma}^\dagger a_{j\sigma} \\ &\quad + \text{dot double empty/filling terms} \\ &\quad + \text{spin-independent lead-scattering terms.} \end{aligned} \quad (\text{A2})$$

The first term resembles the Kondo model. The spin of the QD $\mathbf{S}_i = \sum_{\sigma\sigma'} a_{i\sigma}^\dagger \boldsymbol{\sigma}_{\sigma\sigma'} a_{i\sigma'}$ couples to the band spin $\mathbf{s}_{kq} = \sum_{\sigma\sigma'} c_{k\sigma}^\dagger \boldsymbol{\sigma}_{\sigma\sigma'} c_{k\sigma'}$. The coupling strength is given by $J_{kq}^i = t_{i,q}^* t_{i,k} \left[\frac{1}{\varepsilon_k - \varepsilon_i} - \frac{1}{\varepsilon_k - \varepsilon_i - U_i} + \frac{1}{\varepsilon_q - \varepsilon_i} - \frac{1}{\varepsilon_q - \varepsilon_i - U_i} \right]$. The second term describes a direct tunneling of one QD electron to another dot with the effective coupling strength $A_{ij}^k = t_{i,k}^* t_{j,k} \left[\frac{1 - n_{i\bar{\sigma}}}{\varepsilon_k - \varepsilon_i} + \frac{n_{i\bar{\sigma}}}{\varepsilon_k - \varepsilon_i - U_i} + \frac{1 - n_{j\bar{\sigma}}}{\varepsilon_k - \varepsilon_j} + \frac{n_{j\bar{\sigma}}}{\varepsilon_k - \varepsilon_j - U_j} \right]$, with $\bar{\sigma}$ denoting the opposite spin orientation of σ . This term can also lead to a spin exchange in fourth order, so it is not negligible. The further parts of Eq. (A2) include processes which change the occupation of one QD by two electrons and spin-independent scattering of continuum electrons at one dot.

APPENDIX B: SECOND SCHRIEFFER-WOLFF TRANSFORMATION

For the second Schrieffer-Wolff transformation, the procedure is very similar, using the ansatz for iS_2 that resembles the second order part of the interaction term, derived by the first transformation. However, as one is, in the end, interested in the fourth-order parts of the Hamiltonian, which couple two QD spins and conserve the QD occupation number, one only needs to consider the first two parts of Eq. (A2). The generator for the transformation therefore can be written as $iS_2 = iS_2^{(a)} + iS_2^{(b)}$, with

$$\begin{aligned} iS_2^{(a)} &= \sum_{i,k,q,\sigma} \frac{1}{\varepsilon_k - \varepsilon_q} J_{kq}^i \mathbf{S}_i \cdot \mathbf{s}_{kq}, \\ iS_2^{(b)} &= \frac{-1}{2} \sum_{ij,k,\sigma} \frac{1}{\varepsilon_i + U_i n_{i\bar{\sigma}} - \varepsilon_j - U_j n_{j\bar{\sigma}}} A_{ij}^k a_{i\sigma}^\dagger a_{j\sigma}. \end{aligned} \quad (\text{B1})$$

The other second-order terms finally drop out in the end, when the Hamiltonian is projected on the subspace of single-occupied QDs. For the regrouping of terms in Eqs. (5)–(9), one needs the symmetry of the expressions under the replacements $1 \leftrightarrow 2$ and $k \leftrightarrow q$.

*Present address: AREVA NP GmbH, Erlangen, Germany.

†Corresponding author: guido.burkard@uni-konstanz.de

¹D. Loss and D. P. DiVincenzo, *Phys. Rev. A* **57**, 120 (1998).

²R. Hanson, L. P. Kouwenhoven, J. R. Petta, S. Tarucha, and L. M. K. Vandersypen, *Rev. Mod. Phys.* **79**, 1217 (2007).

³A. H. Castro-Neto, F. Guinea, N. M. R. Peres, K. S. Novoselov, and A. K. Geim, *Rev. Mod. Phys.* **81**, 109 (2009).

⁴B. Trauzettel, D. V. Bulaev, D. Loss, and G. Burkard, *Nature Phys.* **3**, 192 (2007); e-print [arXiv:cond-mat/0611252](https://arxiv.org/abs/cond-mat/0611252).

⁵N. Tombros, C. Jozsa, M. Popinciuc, H. T. Jonkman, and B. J. van Wees, *Nature* **448**, 571 (2007).

⁶S. Sahoo, T. Kontos, J. Furer, C. Hoffmann, Matthias Gräber, A. Cottet, and C. Schönenberger, *Nature Phys.* **1**, 99 (2005).

⁷V. B. Shenoy, *Phys. Rev. B* **71**, 125431 (2005).

⁸K. S. Novoselov, A. K. Geim, S. V. Morozov, D. Jiang, M. I. Katsnelson, I. V. Grigorieva, S. V. Dubonos, and A. A. Firsov, *Nature* **438**, 197 (2005).

⁹M. I. Katsnelson, K. S. Novoselov, and A. K. Geim, *Nature Phys.* **2**, 620 (2006).

¹⁰A. V. Rozhkov, G. Giavaras, Yu. P. Bliokh, V. Freilikher, and F. Nori, *Phys. Rep.* **503**, 77 (2011).

- ¹¹C. Stampfer, J. Güttinger, F. Molitor, D. Graf, T. Ihn, and K. Ensslin, *Appl. Phys. Lett.* **92**, 012102 (2008).
- ¹²P. G. Silvestrov and K. B. Efetov, *Phys. Rev. Lett.* **98**, 016802 (2007).
- ¹³L. Brey and H. A. Fertig, *Phys. Rev. B* **73**, 235411 (2006).
- ¹⁴G. Burkard, D. Loss, and D. P. DiVincenzo, *Phys. Rev. B* **59**, 2070 (1999).
- ¹⁵A. Imamoglu, D. D. Awschalom, G. Durkard, D. P. DiVincenzo, D. Loss, M. Sherwin, and A. Small, *Phys. Rev. Lett.* **83**, 4204 (1999).
- ¹⁶M. A. Ruderman and C. Kittel, *Phys. Rev.* **96**, 99 (1954); T. Kasuya, *Prog. Theor. Phys.* **16**, 45 (1956); K. Yosida, *Phys. Rev.* **106**, 893 (1957); J. H. Van Vleck, *Rev. Mod. Phys.* **34**, 681 (1962).
- ¹⁷K. W.-K. Shung, *Phys. Rev. B* **34**, 979 (1986).
- ¹⁸G. Bastard and C. Lewiner, *Phys. Rev. B* **20**, 4256 (1979).
- ¹⁹B. Wunsch, T. Stauber, F. Sols, and F. Guinea, *New J. Phys.* **8**, 318 (2006).
- ²⁰S. Saremi, *Phys. Rev. B* **76**, 184430 (2007).
- ²¹E. H. Hwang and S. Das Sarma, *Phys. Rev. Lett.* **101**, 156802 (2008).
- ²²V. K. Dugaev, V. I. Litvinov, and J. Barnas, *Phys. Rev. B* **74**, 224438 (2006).
- ²³T. Ando, *J. Phys. Soc. Jpn.* **75**, 074716 (2006).
- ²⁴D. N. Aristov, *Phys. Rev. B* **55**, 8064 (1997).
- ²⁵V. I. Litvinov and V. K. Dugaev, *Phys. Rev. B* **58**, 3584 (1998).
- ²⁶T. Balcerzak, *J. Magn. Magn. Mater.* **310**, 1651 (2007).
- ²⁷Z. Bąk, *Solid State Commun.* **118**, 43 (2001).
- ²⁸P. Durganandini, *Phys. Rev. B* **74**, 155309 (2006).
- ²⁹C. H. Ziener, S. Glutsch, and F. Bechstedt, *Phys. Rev. B* **70**, 075205 (2004).
- ³⁰E. Bauer, *J. Adv. Phys.* **40**, 417 (1991).
- ³¹P. Schlottmann, *Phys. Rev. B* **62**, 10067 (2000).
- ³²C. Proetto and A. López, *Phys. Rev. B* **25**, 7037 (1982).
- ³³P. Coleman, *Lectures on the Physics of Highly Correlated Electron Systems VI*, edited by F. Mancini (American Institute of Physics, New York, 2002), p. 79; e-print [arXiv:cond-mat/0206003](https://arxiv.org/abs/cond-mat/0206003).
- ³⁴C. Proetto and A. Lopez, *Phys. Rev. B* **24**, 3031 (1981).
- ³⁵A. Singh, A. Datta, S. K. Das, and V. A. Singh, *Phys. Rev. B* **68**, 235208 (2003).
- ³⁶J. Zaanen and A. M. Oleś, *Phys. Rev. B* **37**, 9423 (1988).
- ³⁷D. Ihle and M. Kasner, *Phys. Rev. B* **42**, 4760 (1990).
- ³⁸N. Grewe and H. Keiter, *Phys. Rev. B* **24**, 4420 (1981).
- ³⁹E. Kolley, W. Kolley, and R. Tietz, *Phys. Status Solidi B* **204**, 763 (1997).
- ⁴⁰T. Minh-Tien, *Physica C* **223**, 361 (1994).
- ⁴¹C. Sanchez-Castro, B. R. Cooper, and K. S. Bedell, *Phys. Rev. B* **51**, 12506 (1995).
- ⁴²B. Cornut and B. Coqblin, *Phys. Rev. B* **5**, 4541 (1972).
- ⁴³R. Siemann and B. R. Cooper, *Phys. Rev. Lett.* **44**, 1015 (1980).
- ⁴⁴B. Coqblin and J. R. Schrieffer, *Phys. Rev.* **185**, 847 (1969).
- ⁴⁵E. Kolley, W. Kolley, and R. Tietz, *J. Phys. Condens. Matter* **4**, 3517 (1992).
- ⁴⁶J. R. Schrieffer and P. A. Wolff, *Phys. Rev.* **149**, 491 (1966).
- ⁴⁷H. Bruus and K. Flensberg, *Many-Body Quantum Theory in Condensed Matter Physics: An Introduction* (Oxford University Press, Oxford, 2004).
- ⁴⁸A. C. Hewson, *The Kondo Problem to Heavy Fermions* (Cambridge University Press, Cambridge, 2003).
- ⁴⁹G. D. Mahan, *Many Particle Physics* (Plenum Press, New York, 1991).
- ⁵⁰E. Kolley, W. Kolley, and R. Tietz, *J. Phys. Condens. Matter* **10**, 657 (1998).
- ⁵¹One could be tempted to assume, that the separation of the interaction terms in Eq. (4) resembles the distinction of different types of physical interactions. This appears not to be the case.
- ⁵²P. Coleman and N. Andrei, *J. Phys. C* **19**, 3211 (1986).
- ⁵³Q. Zhang and P. M. Levy, *Phys. Rev. B* **34**, 1884 (1986).
- ⁵⁴L. Brey and H. A. Fertig, *Phys. Rev. B* **75**, 125434 (2007).
- ⁵⁵M. Y. Han, B. Ozyilmaz, Y. Zhang, and P. Kim, *Phys. Rev. Lett.* **98**, 206805 (2007).